2002-01-1705

The Effect of Oxygenates on Diesel Engine Particulate Matter

A. S. (Ed) Cheng and Robert W. Dibble
University of California, Berkeley

Bruce A. Buchholz
Lawrence Livermore National Laboratory

ABSTRACT

A summary is presented of experimental results obtained from a Cummins B5.9 175 hp, direct-injected diesel engine fueled with oxygenated diesel blends. The oxygenates tested were dimethoxy methane (DMM), diethyl ether, a blend of monoglyme and diglyme, and ethanol. The experimental results show that particulate matter (PM) reduction is controlled largely by the oxygen content of the blend fuel. For the fuels tested, the effect of chemical structure was observed to be small. Isotopic tracer tests with ethanol blends reveal that carbon from ethanol does contribute to soot formation, but is about 50% less likely to form soot when compared to carbon from the diesel portion of the fuel.

Numerical modeling was carried out to investigate the effect of oxygenate addition on soot formation. This effort was conducted using a chemical kinetic mechanism incorporating n-heptane, DMM and ethanol chemistry, along with reactions describing soot formation. Results show that oxygenates reduce the production of soot precursors (and therefore soot and PM) through several key mechanisms. The first is due to the natural shift in pyrolysis and decomposition products. In addition, high radical concentrations produced by oxygenate addition promote carbon oxidation to CO and CO_2, limiting carbon availability for soot precursor formation. Additionally, high radical concentrations (primarily OH) serve to limit aromatic ring growth and soot particle inception.

INTRODUCTION

Previous studies have shown that diesel engines operating on neat oxygenated fuels produce virtually no particulate matter (PM) emissions [1-6]. However, many oxygenates have fuel properties that make them unattractive as a diesel fuel and some (e.g., dimethyl ether (DME)) require highly modified or even redesigned fuel delivery systems.

These disadvantages can be overcome by using oxygenates as a blending agent for conventional diesel fuel. Oxygenated diesel blends have been shown to dramatically reduce PM emissions from diesel engines, to an extent (% reduction) far greater than their amount of addition (% of fuel by volume or mass) [7-26]. The PM reductions are achieved with little or no change to NO_x emissions, resulting in a favorable shift in the NO_x-PM tradeoff curve. With a fuel-induced reduction in PM, engine modifications can be subsequently employed to reduce NO_x, with the overall effect being a simultaneous reduction in both pollutants. This is illustrated conceptually in Figure 1.

Beyond the emissions benefits, oxygenated diesel blends can help to reduce foreign oil dependence and

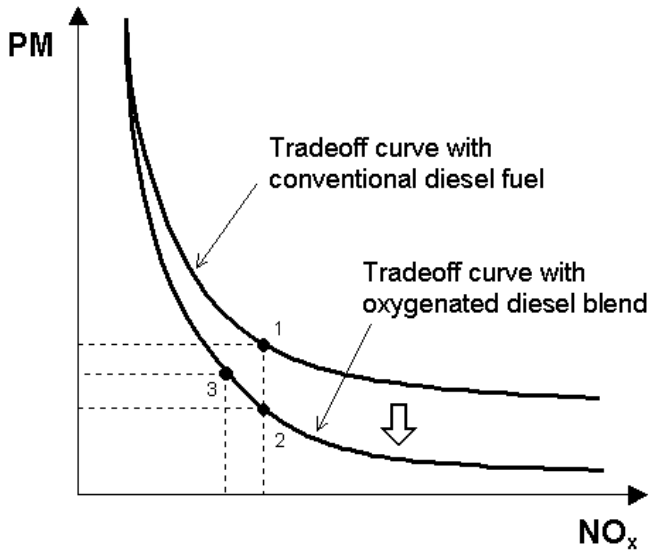

Figure 1. Oxygenated diesel blends produce a shift in the NO_x-PM tradeoff curve. The effect of the fuel change might result a movement from Point 1 to Point 2 in the figure. Subsequent use of engine modifications for NO_x control could then move emissions along the new tradeoff curve to a level represented by Point 3.

promote the use of renewable energy sources. A number of oxygenates can be produced from non-petroleum sources. For example, dimethoxy methane (DMM) and DME can be manufactured from gas-to-liquids processes using natural gas as the feedstock [27]. Glycol ethers such as monoglyme and diglyme can be derived using a syngas process with coal as the feedstock [28]. Certain oxygenates can also be developed as renewable fuels. The most common is ethanol, which can be produced from corn or other biomass. Such bio-derived ethanol can be further manufactured into other oxygenates, such as diethyl ether (DEE).

While the benefits of oxygenated diesel blends are evident, a thorough understanding of the mechanisms that bring about the reductions in PM are not. Many researchers have indicated that fuel oxygen content is the main factor affecting PM emissions. For example, the results of Miyamoto et al. are often cited which show a decrease in Bosch smoke number that is well correlated to fuel oxygen content, with smoke levels becoming essentially zero at an oxygen content of approximately 30% by weight (mass) [13]. However, others have concluded that there are important differences depending on the chemical structure or volatility of a given oxygenate [7, 11, 20, 22]. To further investigate the mechanisms, a number of investigators have carried out numerical modeling of the chemical kinetics in the primary soot formation region [29-33]. These studies provide additional insight into the nature of PM reduction with oxygenated diesel blends.

The current paper has two objectives. The first is to present a summary of experimental results obtained for a variety of oxygenated blends using a Cummins B5.9 175 hp, direct-injected (DI) diesel engine. A number of conclusions are drawn based on the aggregate experimental data. The second objective is to carry out numerical simulations of the effect of oxygenates on soot precursor formation and soot particle inception. This effort was conducted using a chemical kinetic mechanism incorporating n-heptane, DMM and ethanol chemistry, along with reactions describing soot formation. The ultimate goal is to identify the factors that govern PM reductions, so that specific criteria can be used to select the most suitable oxygenated blend fuels for diesel engines.

SUMMARY AND DISCUSSION OF PREVIOUS EXPERIMENTAL RESULTS

The authors have previously presented experimental results from oxygenated blend tests using DMM, DEE, a blend of monoglyme and diglyme called Cetaner, and ethanol [24-26]. The chemical structures and selected properties of these fuels are shown in Table 1. The engine tests were conducted on a 1993 Cummins B5.9 175 hp, 6-cylinder, turbocharged and aftercooled, DI diesel engine. Fuel injection was mechanically governed, although the injection pump was capable of relatively high injection pressures of up to 115 MPa.

Table 1. Chemical structure and selected properties of oxygenated fuels tested.

Fuel component	Chemical Formula	Oxygen content (mass%)	Boiling point (°C)	Heating value (MJ/L)
Dimethoxy methane (DMM)	$CH_3OCH_2OCH_3$	42.1	42	20.2
Diethyl ether (DEE)	$CH_3CH_2OCH_2CH_3$	21.6	34	24.1
Cetaner = 20% monoglyme + 80% diglyme	$CH_3O(CH_2)_2OCH_3$ $CH_3O(CH_2)_2O(CH_2)_2OCH_3$	35.5 35.8	85 162	25.2 26.6
Ethanol	C_2H_5OH	34.7	78	21.2
Diesel	various	—	173-360	35.4

Figure 2 presents a summary of the PM reductions achieved with all of the oxygenated blends tested, relative to the baseline diesel fuels. The figure shows modal-averaged data for steady-state tests run with each of the fuels. The reader is referred to references 24-26 for a detailed description of the experimental procedures and results.

Within the experimental uncertainty, the data does suggest that the oxygen content of a given fuel blend is the predominant factor affecting its ability to reduce PM emissions. Changes in thermophysical properties of the test fuels (cetane number, volatility, energy density) certainly would have affected fuel injection and vaporization, ignition delay times, and heat release rates. Oxygenates with lower oxygen content (within the oxygenate itself) also required higher concentrations to produce a given oxygen level in the blended fuel. This served to displace more of the aromatics and sulfur contained in the baseline fuel and enhance the amount of PM reduction. However, all of these effects appear to

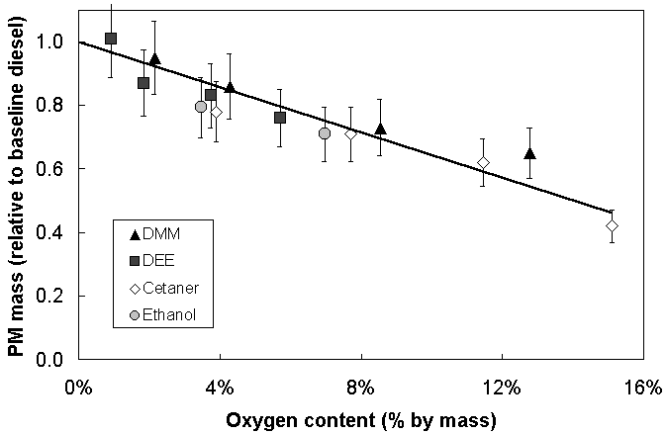

Figure 2. Experimental results of relative PM mass versus oxygen content for four types of oxygenated blend fuels.

have a smaller impact on PM than the blended fuel's oxygen content.

In addition, for the fuels tested, the effect of chemical structure was observed to be small. The oxygenates DEE, Cetaner, and ethanol contain C-C bonds, while DMM does not. The suggestion has been made that an oxygenate that lacks any C-C bonds is less likely to contribute to soot formation and PM mass as it cannot readily form important soot precursors such as acetylene (C_2H_2). However, the experimental data does not support this theory; DMM in fact appeared to be slightly less effective at reducing PM than the other oxygenates. It should be noted however that oxygenates with a wide variety of chemical structures were not tested. The three ethers and the one alcohol had at most two carbon atoms bonded together. Experimental tests conducted by Hallgren and Heywood showed that oxygenates possessing more complex or partial ring structures (diethyl maleate ($C_8H_{12}O_4$) and propylene glycol monomethyl ether acetate ($C_6H_{12}O_3$)) are much less effective for PM reduction when compared to diglyme [20].

Linear extrapolation of a best-fit line to the aggregate data indicates that oxygenate addition would reduce PM emissions to essentially zero at a oxygen content of 28%. This is in good agreement with the results of Miyamoto et al., although it cannot be stated with certainty that a linear relationship exists beyond the oxygenate levels tested.

The experiments conducted with DMM, DEE and Cetaner were carried out at numerous steady-state test modes (8 or 9 engine speed-load conditions) [24, 25]. Individual modal results revealed that oxygenate addition was more beneficial at high load conditions. At lower load conditions, PM emissions were not significantly reduced and in some cases even increased (relative to the baseline diesel fuel). Two factors likely contributed to this effect. The first is that less fuel is injected at lower power modes and therefore less fuel is burned during the mixing-controlled phase of combustion. Since soot formation occurs primarily during this mixing-controlled phase, the effect of the oxygenates on PM would be less pronounced at these engine modes. In addition, the overall (absolute) level of PM at the lower power modes was small. The oxygenated blends produced higher hydrocarbon (HC) emissions, and the contribution to PM mass from adsorbed or condensed HCs may have countered or overwhelmed a small reduction in inorganic PM mass.

An important observation was obtained from the tests with the ethanol blended fuels [26]. Because oxygenates do not produce PM when used as a neat fuel, it has been theorized that the oxygenates themselves do not participate in soot formation during the combustion of a oxygenated blend. For the ethanol blend experiments, accelerator mass spectrometry

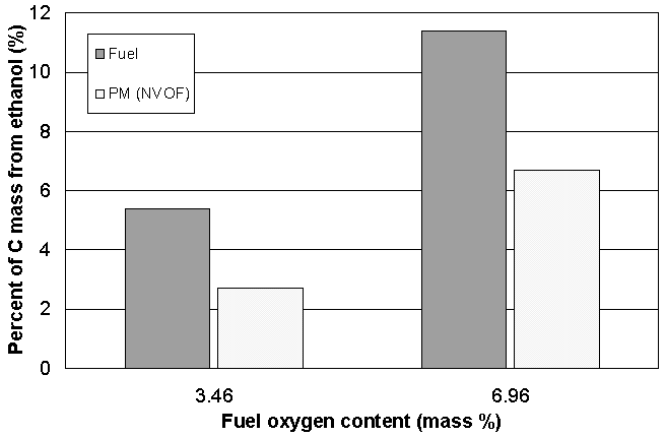

Figure 3. Percent of carbon mass from ethanol in the test fuels and in the non-volatile organic fraction (NVOF) of collected PM.

(AMS) was used to trace the carbon from grain ethanol, which possesses highly elevated carbon-14 radioisotope (^{14}C) levels compared to the petroleum-derived diesel fuel. Results from these tests are shown in Figure 3. As the figure indicates, ethanol carbon does participate in the formation of soot, but is about 50% less likely to form soot when compared to carbon originating from the diesel portion of the fuel.

NUMERICAL MODELING OF SOOT FORMATION

The engine experiments discussed in the previous section provide valuable insight into the nature of PM reduction with oxygenated blend fuels. The results highlight the importance of fuel oxygen content and indicate that combustion chemistry is the major factor governing the ability of oxygenates to reduce diesel PM emissions. To further investigate this chemical effect, it is desirable to conduct numerical modeling of oxygenated fuel combustion under diesel-like conditions.

A comprehensive modeling effort would incorporate a detailed chemical kinetic mechanism for the oxygenated blend fuels along with a complete fluid dynamic description of the combustion chamber environment. However, this is infeasible from a practical standpoint due to current limits in computational power. Because the focus was to be on the chemical aspects of oxygenated fuel combustion, a strategy was employed to investigate detailed chemistry interactions while simplifying the fluid dynamics of the problem. Such a strategy can be justified based on recent insights obtained on the diesel combustion process by Dec and Flynn et al. [29, 33]. Their laser-sheet imaging work suggests that soot formation occurs primarily during the mixing-controlled phase of combustion, in a region between a standing fuel-rich premixed flame and the burning fuel jet's outer diffusion flame (Figure 4). This can be further conceptualized by following a parcel of injected fuel as shown in Figure 5. Fuel initially mixes with air, then is partially consumed in the rich premixed

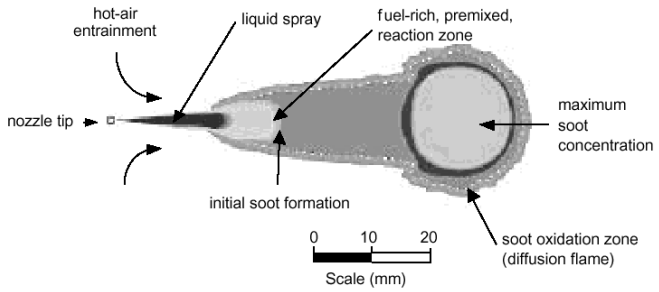

Figure 4. Conceptual view of diesel engine combustion during the mixing-controlled phase (the phase where the majority of soot formation is believed to take place). Soot is formed in the region between the fuel-rich, premixed flame and the outer diffusion flame [33].

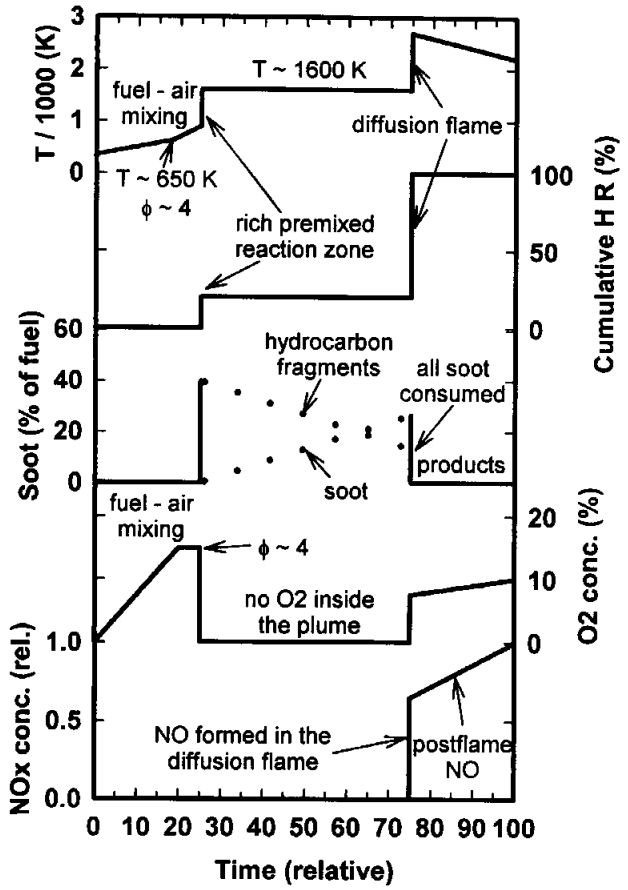

Figure 5. Depiction of processes that take place as a parcel of fuel is injected, becomes partially consumed in the premixed reaction zone, and then encounters the outer diffusion flame sheath [29].

reaction zone, where the fuel-air equivalence ratio is approximately $\phi \cong 4.0$. Soot formation occurs beyond this zone in a region where the products of rich combustion lead to polycyclic aromatic hydrocarbon (PAH) growth and particle inception. All or most of the soot formed is then oxidized upon encountering the diffusion flame sheath, where OH concentrations are high.

The current modeling effort therefore centers on the soot formation region inside the jet (the region between about 25 and 75 on the relative time scale of Figure 5). This region can be represented by a perfectly-mixed (0-D), constant pressure reactor. Flynn et al. [29] and Curran et al. [30, 31] have reported on changes to C_2H_2, ethylene (C_2H_4), and propargyl (C_3H_3) concentrations in this region due to the addition of various oxygenates. More recently, Kitamura et al. [32] has predicted the effect of oxygenates on PAH formation. The current effort utilizes a mechanism that carries the soot chemistry all the way to initial particle inception. The effect of oxygen levels is investigated using two oxygenates: DMM and ethanol. The objective is to study the evolution of soot concentrations within the soot formation region and also to predict soot levels at the location of the diffusion flame.

MECHANISM DEVELOPMENT

The overall reaction mechanism was developed beginning with a mechanism for n-heptane (C_7H_{16}) that included a chemical description of soot formation and oxidation. Although diesel fuel is actually comprised of many different hydrocarbon compounds, n-heptane serves as a good chemical surrogate for diesel and has cetane number similar to that of typical diesel fuels (CN $\cong$ 56) [34].

Reaction chemistry for DMM and ethanol was added to the n-heptane + soot mechanism using data from two other individual mechanisms. The combined reaction mechanism used in the numerical calculations of this paper consists of 159 species and 936 reactions.

N-Heptane + Soot Mechanism

The n-heptane + soot mechanism used was developed by Golovitchev et al. [34, 35] and is derived from the models of Westbrook et al. (n-heptane) [36-41] and Frenklach and Wang (soot) [42-44]. These models have been described extensively in the literature, but a summary of the key processes will be given here.

For the n-heptane chemistry, at the high-temperature conditions of diesel combustion (T > 900 K), initiation steps consist of unimolecular n-heptane decomposition as well as H-atom abstraction. The overall reaction then proceeds primarily through decomposition (β-scission) of the alkyl radicals, although O_2 addition can play an important role at more moderate temperatures (T $\cong$ 900 K).

The smaller gas-phase products of the n-heptane oxidation then serve as the building blocks for aromatic formation and PAH growth. The soot model begins with a series of reactions involving C_2H_2 and molecular hydrogen which lead to the formation of the phenyl radical ($A_1^{\cdot}$). This pathway is shown in Figure 6*a*.

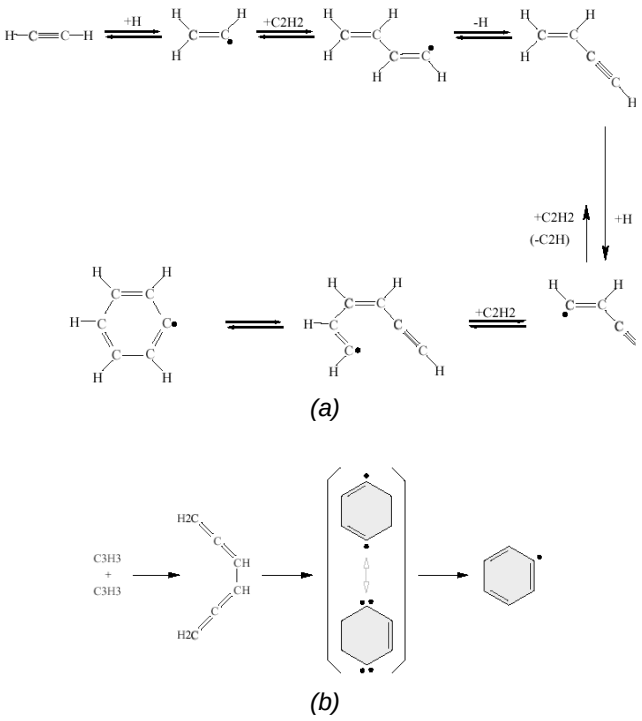

Figure 6. Formation of the phenyl radical from *(a)* reactions involving acetylene (C_2H_2) and *(b)* combination of two propargyl radicals (C_3H_3) [34].

Alternatively, the phenyl radical can be formed from two propargyl radicals (C_3H_3) as shown in Figure 6*b*. Following the formation of the first aromatic ring (A_1 = benzene), reactions involving H-atom abstraction and C_2H_2 addition (the so-called HACA mechanism) lead to aromatic ring growth. This mechanism is as follows:

$$A_i + H \rightarrow A_i^{\bullet} + H_2 \quad (1)$$
$$A_i^{\bullet} + C_2H_2 \rightarrow A_i\dot{C}_2H_2 \quad (2)$$
$$A_i\dot{C}_2H_2 + H \rightarrow A_i\dot{C}_2H + H_2 \quad (3)$$
$$A_i\dot{C}_2H + C_2H_2 \rightarrow A_{i+1} \quad (4)$$

where i represents the number of aromatic rings in a given species. The growth aromatic rings is included up to four-ring species. At that point, a prompt transition to soot (soot inception) is assumed to occur, i.e.,

$$A_4 \rightarrow 16C(s) + 5H_2 \quad (5)$$

To limit aromatic ring growth, oxidation by OH and O_2 is included, using rate parameters from Frenklach and Wang [44].

DMM Mechanism

Chemistry for DMM ($CH_3OCH_2OCH_3$) combustion was considered in the overall reaction mechanism based on the model of Naegeli et al. [45]. Initial reactions of the parent fuel are those of unimolecular decomposition and H-atom abstraction. Additional reactions with radical species produce dimethyl ether (CH_3OCH_3) and methyl formate (CH_3OCHO), which further react to yield radical and smaller species. The methoxy methyl radical (CH_3OCH_2) is believed to play a particularly important role in the DMM kinetics through its reactions with oxygen (O_2) [45]. Also included in the mechanism are reactions that describe formaldehyde (CH_2O) chemistry.

The DMM mechanism was combined with the n-heptane + soot mechanism described above to produce a combined chemical kinetic model that could describe the behavior of DMM blends. In cases where there were duplicate reactions with different rate constants, the reactions from the n-heptane + soot mechanism were retained. This was because the n-heptane chemistry was more detailed and therefore involved a greater number of interdependent reactions that would be impacted by any changes in rate constants. Also, since the soot formation model was developed in conjunction with the n-heptane chemistry, it was desirable to retain as much of this original combination as possible.

Ethanol Mechanism

The chemical kinetics of ethanol (C_2H_5OH) were included in the overall mechanism using reaction data developed by Marinov [46]. Of particular importance in the ethanol chemistry are the reactions that decompose C_2H_5OH to $CH_3 + CH_2OH$, $C_2H_5 + OH$, $CH_3 + CH_2O$, and $CH_3HCO + H$. The evolution of intermediate and product species are also strongly influenced by reactions describing OH attack on the parent fuel. As with the DMM chemistry, ethanol species and reactions were added to the combined reaction mechanism (with the exception of those which would lead to duplication).

Mechanism Validation

Both the n-heptane + soot and ethanol mechanisms have been extensively tested against experimental data from flow reactors, jet-stirred reactors, shock tubes, and rapid compression machines [34, 37, 42, 45, 46]. It was uncertain, however, whether the chemical kinetics described by the original mechanisms would be significantly altered by combining the mechanisms together. To investigate this possibility, model runs were conducted to compare ignition delay times predicted by the combined mechanism to those determined with the original mechanisms. The ignition delay times were computed using a constant volume, adiabatic, well-mixed (0-D) computational code [47].

Results for n-heptane – air mixtures are shown in Figure 7. Figure 7*a* shows the original data from the Golovitchev mechanism, while Figure 7*b* presents results form the current combined model. As the figures indicate, agreement between the two cases is very good. The combined mechanism properly exhibits the negative temperature coefficient (NTC) behavior in the temperature region that is associated with diesel combustion. There are slight differences in predicted ignition delays at lower temperature, fuel-lean conditions

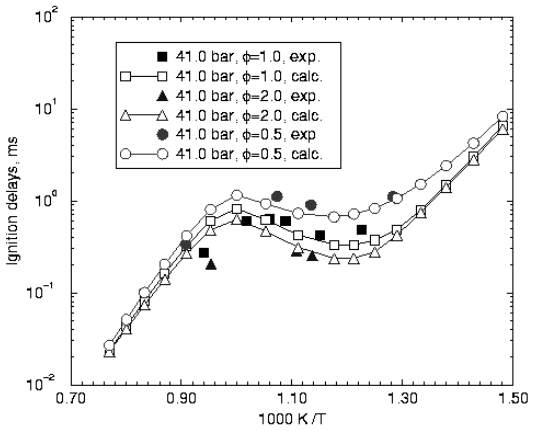

(a)

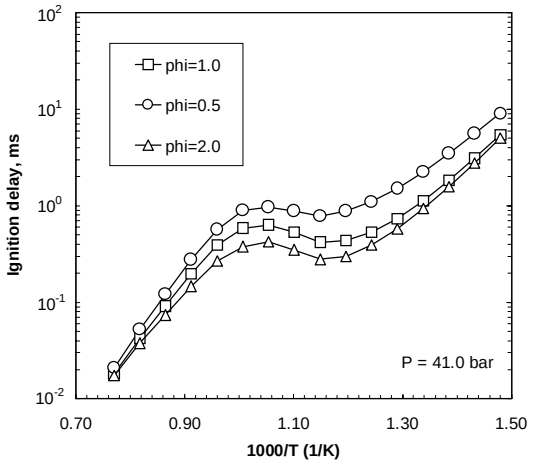

(b)

Figure 7. Mechanism validation for n-heptane – air mixtures. *(a)* Original Golovitchev mechanism results (open symbols) versus experimental data (solid symbols) [34], and *(b)* numerical results using combined mechanism.

(T < 800 K, ϕ = 0.5). However, this would have little impact on the current investigation which models reactions occurring under higher temperature, fuel-rich conditions.

Figure 8 shows comparisons between ignition delay results from the Marinov ethanol mechanism (Figure 8*a*) and results obtained from the combined mechanism (Figure 8*b*). The reactants are a mixture of 2.5% ethanol, 7.5% O_2 and 90% argon (mole fractions). Again, the combined mechanism shows excellent agreement with the original numerical results.

In contrast to the situation for the n-heptane and ethanol mechanisms, the chemical kinetics of the DMM mechanism cannot been rigorously tested due to the lack of experimental data available on the fundamental combustion behavior this fuel. The evolution of pyrolysis products has been measured by Edgar et al. [45] and those results do compare favorably with the numerical results of both the original DMM mechanism and the combined reaction mechanism. However, since

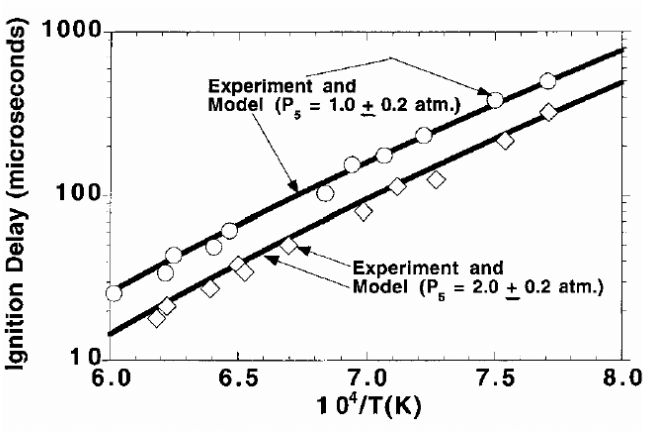

(a)

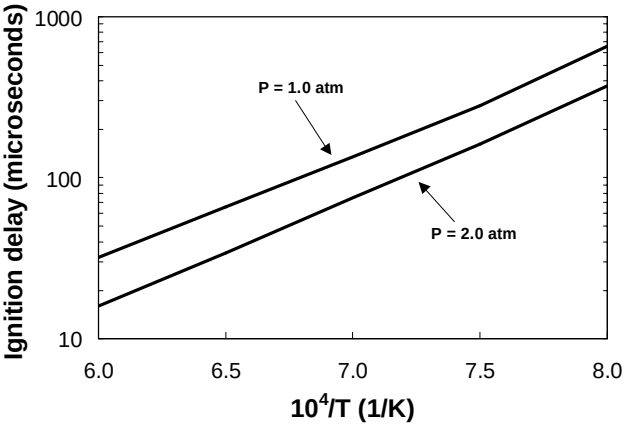

(b)

Figure 8. Mechanism validation for a mixture of 2.5% ethanol, 7.5% O_2, and 90% argon. *(a)* Comparison between Marinov mechanism and experimental results [46], and *(b)* numerical results using combined mechanism.

the mechanism has not been tested against a large number of experimental measurements, the validity of the DMM reaction kinetics cannot be determined with absolute certainty.

COMPUTATIONAL CODE

As previously mentioned, the numerical modeling effort focuses on the fuel-rich soot formation region that can be represented by a homogeneous, constant pressure reactor. Model runs were carried out assuming adiabatic, well-mixed, constant pressure conditions, similar to the strategy employed by Flynn et al. and Curran et al. [29-31]. The computational code utilizes the Chemkin-II interpreter and subroutine package to carry out the chemical kinetic computations and solve the governing conservation equations (Chemkin Interpreter version 3.6 and Chemkin Subroutine Library version 4.9). A full description of the Chemkin software can be found in References 48 and 49.

For all of the computations, an initial temperature of T_i = 1000 K and an initial pressure of P_i = 10 MPa were used. These values are representative of combustion conditions in the Cummins B5.9 engine, as estimated based upon pressure transducer data [50] and analogy to the conditions measured by laser diagnostics in Dec's experimental engine [33]. The initial fuel-air equivalence ratio for all cases was set at ϕ = 4.0, which matches the approximate conditions of the standing premixed flame [29, 33]. During diesel engine combustion, the addition of oxygenates might alter to some extent the equivalence ratio in the mixture of injected fuel and entrained hot air (at a given point from the injector). However, since the standing premixed flame would develop at a location determined in large part by the equivalence ratio (for a given engine), it is fairly reasonable to maintain a constant value for ϕ regardless of the fuel oxygen content. Also, from a modeling standpoint, it was desirable to separate the effect of oxygenated fuel chemistry from any effects arising simply due to differences in equivalence ratio.

RESULTS AND DISCUSSION

The analysis of numerical results focuses on soot concentrations and the precursor species C_2H_2, C_3H_3, and the first aromatic ring A_1. The evolution of these species inside the jet plume varies depending on the particular species under consideration. C_3H_3 is created almost exclusively in the fuel-rich premixed flame, where it experiences a sharp peak in concentration and is then rapidly consumed and converted to other species. This is shown for the case of n-heptane in Figure 9*a*. Also presented in this figure is the concentration profile for C_2H_2, which is seen to rise to its peak at the flame but then gradually falls.

Figure 9*b* shows the concentration profiles for A_1 and for soot, again for the case of n-heptane combustion. A large amount of aromatic formation occurs at the flame zone, due to the high concentrations of precursor species at this location. The concentration of A_1 then increases slightly as it continues to be formed, but eventually decreases as C_2H_2 and C_3H_3 concentrations drop and PAH growth occurs (for the n-heptane case shown in Figure 9*b*, the decrease in A_1 concentration occurs beyond the time scale shown in the figure). The level of soot rises steadily within the jet plume, as is suggested by the conceptual model of Figure 5.

Addition of the oxygenated fuels (DMM and ethanol) does not alter the shapes of the concentration profiles described above, but does affect the magnitude of the peak concentrations and the rate at which soot is formed.

In the plots of Figure 9, the time scale was chosen to extend to about 0.56 ms. This corresponds to a time of 0.50 ms after reaction takes place in the premixed flame

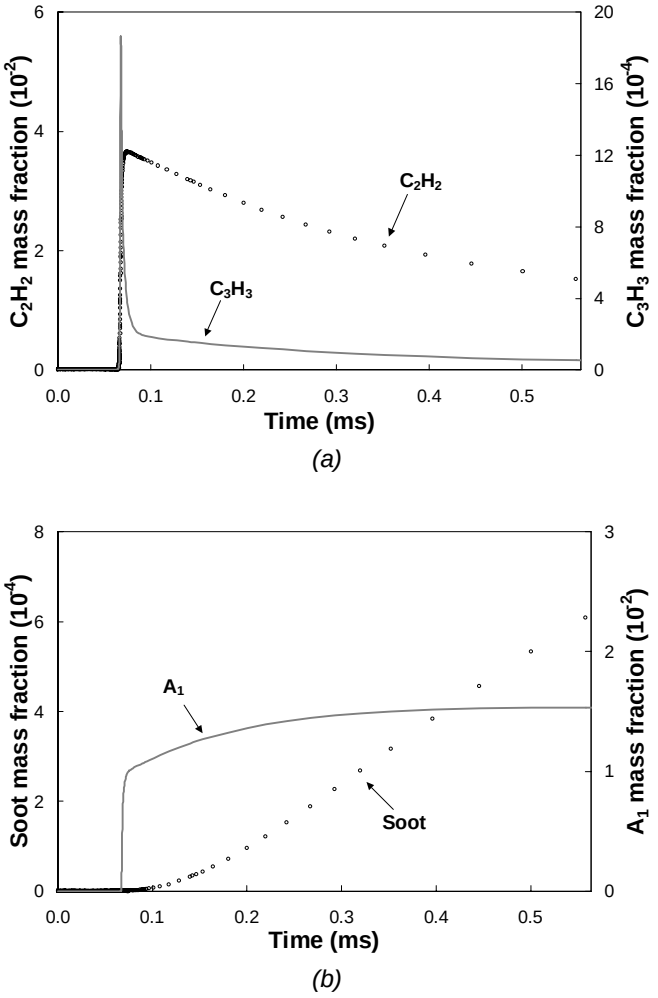

Figure 9. Species concentration profiles for the case of n-heptane (ϕ = 4.0, T_i = 1000 K, P = 10 MPa). *(a)* Acetylene (C_2H_2) and propargyl (C_3H_3) and *(b)* benzene (A_1) and soot.

(about 0.06 ms, as defined by the point where the C_3H_3 concentration reaches its peak). The reasoning behind the use of the 0.5 ms time interval is that it represents the approximate time required for the products of the fuel-rich combustion to travel from the premixed flame to the diffusion flame sheath [29] (about 5 crank angle degrees (CAD) at an engine speed of 1600 rpm). Identified soot concentrations at the location of the diffusion flame can then be used as a predictor for exhaust soot levels, based upon the following assumptions: (1) the diffusion flame oxidizes most but not quite all of the soot created within the plume, and/or (2) quenching of the reaction during the expansion stroke causes the last parcels of injected fuel to produce soot that is not subsequently oxidized.

Effect of DMM Addition

The gradual replacement of n-heptane by DMM in the numerical model results in notable changes to the peak concentrations of soot precursors at the premixed reaction zone. This subsequently alters the nature of aromatic formation and PAH growth and serves to

suppress soot particle inception. Figure 10 shows the peak concentrations of C_2H_2, C_3H_3 and A_1 plotted with respect to oxygen content, as DMM is added to the fuel. As the figure shows, peak C_2H_2 and peak A_1 concentrations steadily decline with DMM addition. Peak C_3H_3 concentrations are not significantly affected at lower oxygen levels, but decrease as oxygen content is increased beyond 10% by mass.

Figure 11 presents the predicted soot concentrations at the location of the diffusion flame (relative to the n-heptane only case), based on the 0.5 ms time-of-flight assumption discussed above. Note that the exact time interval selected would not dramatically affect the relative mass concentration results since soot forms proportionally over time (Figure 12). The data in Figure 11 shows that computed soot concentrations decline in a linear fashion up to a fuel oxygen content of about 17% (corresponding to 40% DMM by volume, or DMM-40). Beyond that point, soot levels continue to decrease with DMM addition until virtually no soot is produced (at a fuel oxygen content between 35% and 40%).

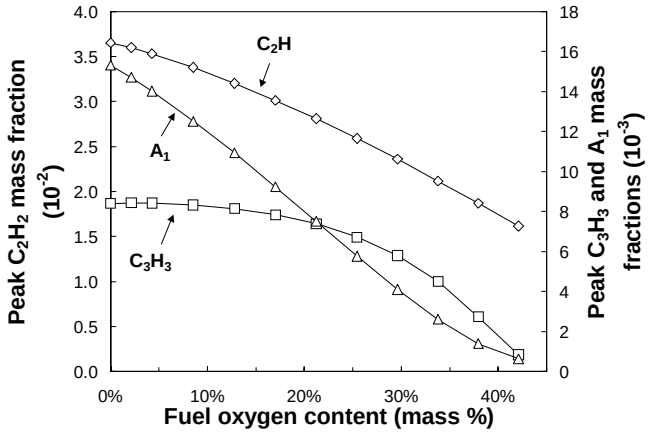

Figure 10. Changes to peak soot precursor concentrations due to DMM addition (ϕ = 4.0, T_i = 1000 K, P = 10 MPa).

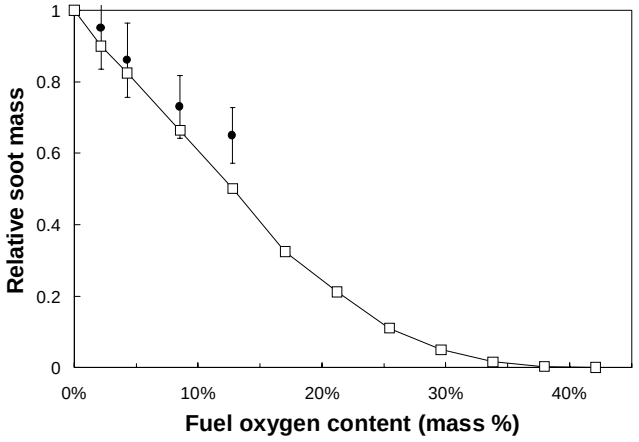

Figure 11. Predicted soot mass concentrations at the location of the diffusion flame for DMM addition (ϕ = 4.0, T_i = 1000 K, P = 10 MPa). Solid symbols represent experimental data for PM mass.

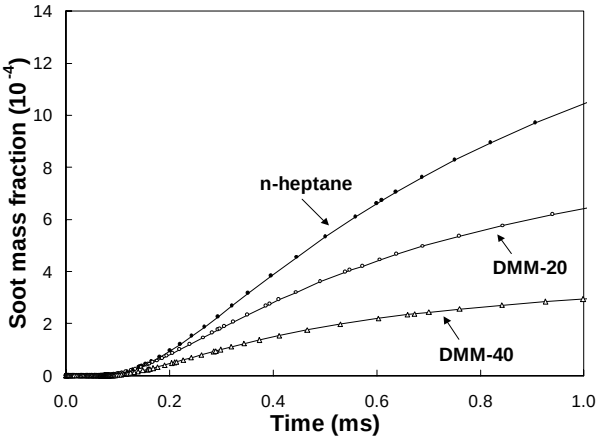

Figure 12. Evolution of soot concentrations within the burning jet plume for different levels of DMM addition (ϕ = 4.0, T_i = 1000 K, P = 10 MPa).

Figure 11 also shows the experimental data obtained with the DMM blend fuels using the Cummins B5.9 engine (represented by the solid circles). The numerical simulation reveals a trend similar to that of the experimental data, but would overpredict the amount of PM reduction achieved during actual diesel combustion. This observation is not surprising considering the simplifications made by the model and the fact that additional processes contributing to PM mass (both within the combustion chamber and during exhaust and dilution) are not considered.

Effect of Ethanol Addition

The addition of ethanol to n-heptane in the numerical model produced similar trends to those observed with DMM. Figure 13 shows the results for peak soot precursor levels as oxygen content is increased. The effect of ethanol on peak C_3H_3 concentrations is nearly identical to that for DMM. However, based on the model results, ethanol is more effective at reducing peak concentrations of C_2H_2 and A_1. As a consequence,

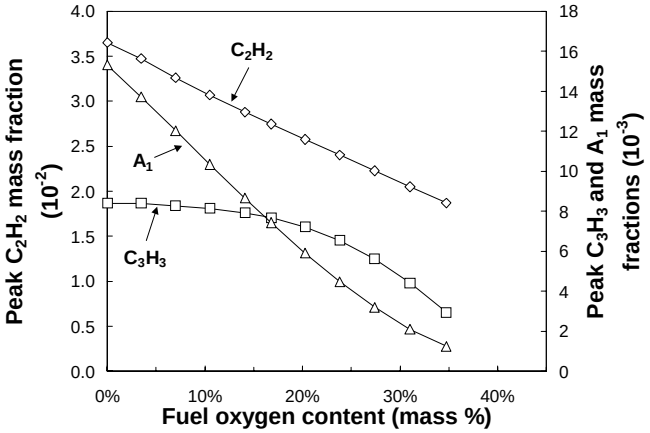

Figure 13. Changes to peak soot precursor concentrations due to ethanol addition (ϕ = 4.0, T_i = 1000 K, P = 10 MPa).

ethanol reduced soot concentrations more effectively than DMM for equivalent levels of oxygen addition (Figure 14). Soot production was completely suppressed at a fuel oxygen content around 35%. As was the case with DMM, the magnitude of the soot formation curve decreased with ethanol addition, but the general shape of the curve was not altered. This is illustrated in Figure 15.

Comparison with the experimental results from the B5.9 engine (Figure 16) show that the model again predicts reductions in soot concentrations that are more pronounced than measured PM reductions. However, the model does accurately reproduce the experimental observation that ethanol appears more effective than DMM at lowering PM (as a function of fuel oxygen content). This suggests that the current model is capable of evaluating the relative PM reduction potential of different oxygenated fuels.

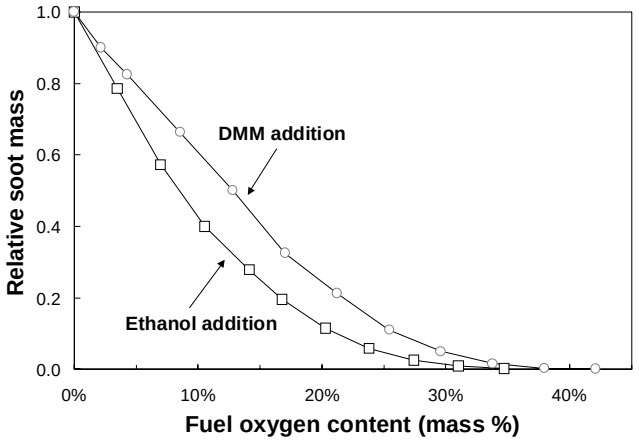

Figure 14. Comparison of predicted soot precursor concentrations at the diffusion flame for ethanol addition and DMM addition (ϕ = 4.0, T_i = 1000 K, P = 10 MPa).

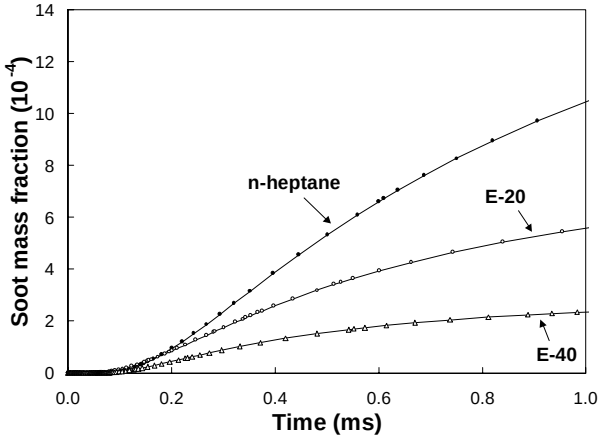

Figure 15. Evolution of soot concentrations within the burning jet plume for different levels of ethanol addition (ϕ = 4.0, T_i = 1000 K, P = 10 MPa).

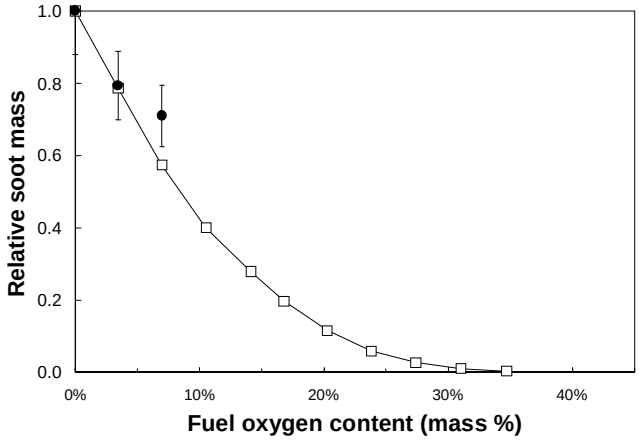

Figure 16. Predicted soot mass concentrations at the location of the diffusion flame for ethanol addition (ϕ = 4.0, T_i = 1000 K, P = 10 MPa). Solid symbols represent experimental data for PM mass.

Discussion of the Oxygenate Effect

It is evident from the numerical modeling of oxygenate addition that the key factor affecting soot formation is the nature of the reaction products of the fuel-rich premixed flame. The relative concentrations of species in this zone controls the subsequent processes of aromatic ring formation, PAH growth, and soot particle inception.

A direct effect on product species in the premixed flame zone arises from the difference in pyrolysis products for n-heptane and for the oxygenates DMM and ethanol. N-heptane decomposes primarily via β-scission and produces small carbon chain species that readily lead to soot precursors. In contrast, DMM lacks any C-C bonds and can only create soot precursors through a more lengthy reaction pathway. Ethanol contains a single C-C bond and cannot immediately form any C_3 precursor species, but it is capable of producing C_2 species. However, since the C-O bond strength is greater than that of the C-C bond, decomposition of ethanol would in fact tend to yield single carbon species rather than the C_2 species that could eventually serve as building blocks for aromatic formation.

An additional, and perhaps more important effect of oxygenate addition is revealed from an investigation of individual species concentrations in the premixed reaction zone. Concentrations of radicals such as O, OH, and HCO are increased, sometimes dramatically, as oxygen addition takes place. The impact that this increase in radical concentrations has on soot formation is two-fold. First, large O and OH concentrations promote oxidation to CO and CO_2 within the flame and reduce the amount of carbon available for the production of soot precursor species. Formation of high amounts of HCO results in a similar effect, as HCO readily is converted to CO or CO_2 through a single reaction step. Secondly, an increased concentration of radicals, primarily OH, in the post-premixed flame soot formation

region, serves to suppress particle inception by oxidizing aromatic species and limiting PAH growth. In fact, one of the main differences between ethanol addition and DMM addition is that peak OH radical concentrations were observed to increase much more dramatically with the addition of ethanol (Figure 17). This is believed to be one of the primary reasons that ethanol is more effective than DMM at reducing soot concentrations. The impact of DMM addition was much greater for the HCO radical, which lowers soot precursor concentrations but would not contribute as significantly in limiting subsequent aromatic ring growth.

Because the production of CO and CO_2 limits carbon participation in soot formation reactions, the O/C ratio of a given mixture of oxygenated fuel and air (at a fixed stoichiometry, in this case ϕ = 4.0) appears to serve as a better parameter than fuel oxygen content for assessing a fuel's soot reduction potential. This illustrated in Figure 18.

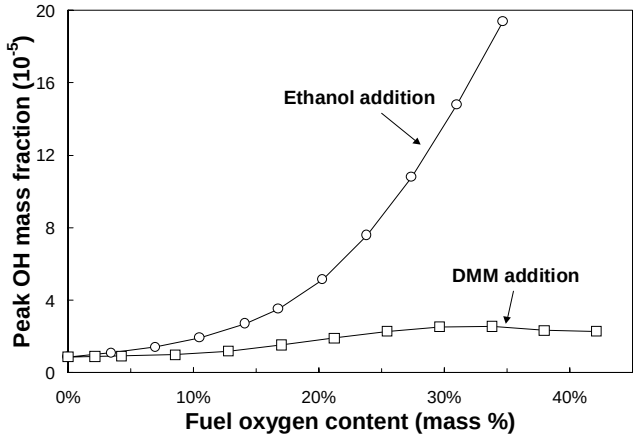

Figure 17. Comparison of peak OH concentrations for ethanol addition and DMM addition (ϕ = 4.0, T_i = 1000 K, P = 10 MPa).

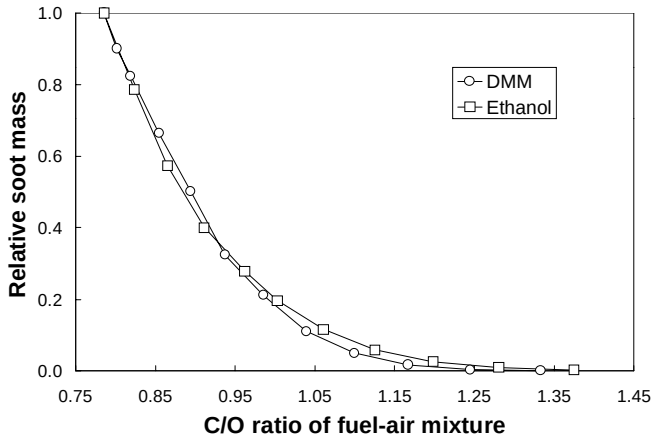

Figure 18. Predicted soot precursor concentrations for ethanol and DMM addition, plotted with respect to the C/O ratio of the overall fuel-air mixture (ϕ = 4.0, T_i = 1000 K, P = 10 MPa).

SUMMARY AND CONCLUSIONS

Experimental results from a Cummins B5.9 diesel operated with oxygenated diesel blends showed that PM reduction levels were influenced largely by the oxygen content of the blend fuel. For the fuels tested, the effect of chemical structure on measured PM mass was observed to be small. Individual modal variations in the effectiveness of oxygenate addition were attributed to the smaller absolute levels of PM at lower load conditions, as well as the contribution of condensed or adsorbed hydrocarbons at those modes. Isotopic tracer tests with ethanol blends revealed that carbon from ethanol did contribute to soot formation, but was about 50% less likely to form soot when compared to carbon from the diesel portion of the fuel.

Numerical modeling results show that oxygenates reduce the production of soot precursors (and therefore soot and PM) through several key mechanisms. The first is due to the natural shift in pyrolysis and decomposition products as oxygen-containing fuels displace the long carbon chains present in conventional diesel fuel. In addition, high radical concentrations produced by the oxygenates in the premixed flame zone promote the oxidation of carbon to CO and CO_2, limiting carbon availability for soot precursor formation. An additional effect of high radical concentrations occurs after the premixed flame, where increased OH concentrations limit aromatic ring growth and soot particle inception.

Differences were observed in the two oxygenates evaluated in the numerical modeling (DMM and ethanol). Ethanol showed larger reductions in soot concentrations for equal amounts of oxygen addition. This was believed to be in large part due to the greater amount of OH radicals produced by ethanol addition. Because of the importance of CO and CO_2 production in limiting carbon availability for soot formation, the O/C ratio of fuel-air mixtures was found to be a parameter that is well correlated to the ability of an oxygenated fuel to reduce soot particle concentrations.

ACKNOWLEDGMENTS

Some of this work was performed under the auspices of the U.S. Department of Energy by University of California Lawrence Livermore National Laboratory under Contract No. W-7405-Eng-48. Support was provided by LLNL Laboratory Directed Research and Development grant 01-ERI-007.

REFERENCES

1. Akasaka, Y., T. Sasaki, S. Kato and S. Onishi. "Evaluation of Oxygenated Fuel by Direct Injection Diesel and Direct Fuel Injection Impingement

Diffusion Combustion Diesel Engines," SAE Technical Paper 901566, 1990.
2. Fleisch, T., C. McCarthy, A. Basu, C. Udovich, P. Charbonneau, W. Slodowske, S.-E. Mikkelsen and J. McCandless. "A New Clean Diesel Technology: Demonstration of ULEV Emissions on a Navistar Diesel Engine Fueled with Dimethyl Ether," SAE Technical Paper 950061, 1995.
3. Wong, G., B. L. Edgar, T. J. Landheim, L. P. Amlie and R. W. Dibble. "Low Soot Emission from a Diesel Engine Fueled with Dimethyl and Diethyl Ether," WSS/CI Paper 95F-162, October 1995.
4. Sorenson, S. C. and S.-E. Mikkelsen. "Performance and Emissions of a 0.273 Liter Direct Injection Diesel Engine Fueled with Neat Dimethyl Ether," SAE Paper 950064.
5. Mikkelsen, S.-E., J. B. Hansen and S. C. Sorenson. "Progress with Dimethyl Ether," International Alternative Fuels Conference, Milwaukee, WI, June 25-28, 1996.
6. Kajitani, S., Z. L. Cheng, M. Konno and K. T. Rhee. "Engine Performance and Exhaust Characteristics of Direct-Injection Diesel Engine Operated with DME," SAE Technical Paper 972973, 1997.
7. Liotta, Jr., F. J. and D. M. Montalvo. "The Effect of Oxygenated Fuels on Emission from a Modern Heavy-Duty Diesel Engine," SAE Technical Paper 932734, 1993.
8. Ullman, T. L., K. B. Spreen and R. L. Mason. "Effects of Cetane Number, Cetane Improver, Aromatics, and Oxygenates on 1994 Heavy-Duty Diesel Engine Emissions," SAE Technical Paper 941020, 1994.
9. Spreen, K. B., T. L. Ullman and R. L. Mason. "Effects of Cetane Number, Aromatics, and Oxygenates on Emissions From a 1994 Heavy-Duty Diesel Engine With Exhaust Catalyst," SAE Technical Paper 950250, 1995.
10. Tsurutani, K., Y. Takei, Y. Fujimoto, J. Matsudaira and M. Kumamoto. "The Effects of Fuel Properties and Oxygenates on Diesel Exhaust Emissions," SAE Technical Paper 952349, 1995.
11. Miyamoto, N., H. Ogawa, T. Arima and K. Miyakawa. "Improvement of Diesel Combustion and Emissions with Addition of Various Oxygenated Agents to Diesel Fuel," SAE Technical Paper 962115, 1996.
12. McCormick, R. L., J. D. Ross and M. S. Graboski. "Effect of Several Oxygenates on Regulated Emissions from Heavy-Duty Diesel Engines," *Environmental Science & Technology*, vol. 31, no. 4, pp. 1114-1150, 1997.Dec, J. E. "A Conceptual Model of DI Diesel Combustion Based on Laser-Sheet Imaging," SAE Technical Paper 970873, 1997.
13. Miyamoto, N., H. Ogawa, N. M. Nurun, K. Obata and T. Arima. "Smokeless, Low NO_x, High Thermal Efficiency, and Low Noise Diesel Combustion with Oxygenated Agents as Main Fuel," SAE Technical Paper 980506, 1998.
14. Maricq, M. M., R. E. Chase, D. H. Podsiadlik, W. O. Siegl and E. W. Kaiser. "The Effect of Dimethoxy Methane Additive on Diesel Vehicle Particulate Emissions," SAE Technical Paper 982572, 1998.
15. Uchida, M. and Y. Akasaka. "A Comparison of Emissions from Clean Diesel Fuels," SAE Technical Paper 1999-01-1121, 1999.
16. Beatrice, C., C. Bertoli, N. Del Giacomo and M.na. Migliaccio. "Potentiality of Oxygenated Synthetic Fuel and Reformulated Fuel on Emissions from a Modern DI Diesel Engine," SAE Technical Paper 1999-01-3595, 1999.
17. Xiao, Z., N. Ladommatos and H. Zhao. "The Effect of Aromatic Hydrocarbons and Oxygenates on Diesel Engine Emissions," *Proc. Instn. Mech. Engrs.*, Vol. 214, Part D, pp. 307-332, 2000.
18. Hess, H. S., A. L. Boehman, P. J. A. Tijm and F. J. Waller. "Experimental Studies of the Impact of Cetaner on Diesel Combustion and Emissions," SAE Technical Paper 2000-01-2886, 2000.
19. Chapman, E., S. V. Bhide, A. L. Boehman, P. J. A. Tijm and F. J. Waller. "Emissions Characteristics of a Navistar 7.3L Turbodiesel Fueled with Blends of Oxygenates and Diesel," SAE Technical Paper 2000-01-2887, 2000.
20. Hallgren, B. E. and J. B. Heywood. "Effects of Oxygenated Fuels on DI Diesel Combustion and Emissions," SAE Technical Paper 2001-01-0648, 2001.
21. Hilden, D. L., J. C. Eckstrom and L. R. Wolf. "The Emissions Performance of Oxygenated Diesel Fuels in a Prototype Diesel Engine," SAE Technical Paper 2001-01-0650, 2001.
22. Yeh, L. I., D. J. Rickeard, J. L. C. Duff, J. R. Bateman, R. H. Schlosberg and R. F. Caers. "Oxygenates: An Evaluation of Their Effects on Diesel Emissions," SAE Technical Paper 2001-01-2019, 2001.
23. Kitagawa, H., T. Murayama, S. Tosaka and Y. Fujiwara. "The Effect of Oxygenated Diesel Fuel Additive on the Reduction of Diesel Exhaust Particulates," SAE Technical Paper 2001-01-2020, 2001.
24. Cheng, A. S. and R. W. Dibble. "Emissions Performance of Oxygenate-in-Diesel Blends and Fischer-Tropsch Diesel in a Compression Ignition Engine," SAE Technical Paper 1999-01-3606, 1999.
25. Cheng, A. S. and R. W. Dibble. "Emissions from a Cummins B5.9 Diesel Engine Fueled with Oxygenate-in-Diesel Blends," SAE Technical Paper 2001-01-2505, 2001.
26. Buchholz, B. A., A. S. Cheng and R. W. Dibble. "Isotopic Tracing of Bio-Derived Carbon from Ethanol-in-Diesel Blends in the Emissions of a Diesel Engine," SAE Techncal Paper (02SFL-12), 2002.
27. Hansen, J. B., B. Voss, F. Joensen and I. D. Siguroardottir. "Large Scale Manufacture of Dimethyl Ether - A New Alternative Diesel Fuel From Natural Gas," SAE Technical Paper 950063, 1995.

28. Hess, H. S., J. Szybist, A. L. Boehman, J. M. Perez, P. J. A. Tijm and F. A. Waller. "Impact of Oxygenated Fuel on Diesel Engine Performance and Emissions," 6th Diesel Engine Emissions Reduction Workshop, San Diego, CA, August 20-24, 2000.
29. Flynn, P. F., R. P. Durrett, G. L. Hunter, A. O. zur Loye, O. C. Akinyemi, J. E. Dec and C. K. Westbrook. "Diesel Combustion: An Integrated View Combining Laser Diagnostics, Chemical Kinetics, and Empirical Validation," SAE Paper 1999-01-0509.
30. Curran, H. J., E. Fisher, P.-A. Glaude, N. M. Marinov, W. J. Pitz and C. K. Westbrook. "Detailed Chemical Kinetic Modeling of Diesel Combustion with Oxygenated Fuels," Fall Meeting of the Western States Section of the Combustion Institute, Irvine, CA, October 25-26, 1999.
31. Curran, H. J., E. M. Fisher, P.-A. Glaude, N. M. Marinov, W. J. Pitz, C. K. Westbrook, D. W. Layton, P. F. Flynn, R. P. Durrett, A. O. zur Loye, O. C. Akinyemi and F. L. Dryer. "Detailed Chemical Kinetic Modeling of Diesel Combustion with Oxygenated Fuels," SAE Technical Paper 2001-01-0653.
32. Kitamura, T., T. Ito, J. Senda and H. Fujimoto. "Detailed Chemical Kinetic Modeling of Diesel Spray Combustion with Oxygenated Fuels," SAE Technical Paper 2001-01-1262.
33. Dec, J. E. "A Conceptual Model of DI Diesel Combustion Based on Laser-Sheet Imaging," SAE Technical Paper 970873, 1997.
34. Golovitchev, V. I., F. Tao and J. Chomiak, "Numerical Investigation of Soot Formation Control at Diesel-Like Conditions by Reduction Fuel Injection Timing," SAE Technical Paper 1999-01-3552.
35. Rente, T., V. I. Golovitchev and I. Denbratt. "Effect of Injection Parameters on Autoignition and Soot Formation in Diesel Sprays," SAE Technical Paper 2001-01-3687.
36. Curran, H. J., P. Gaffuri, W. J. Pitz and C. K. Westbrook. "A comprehensive Modeling Study of n-Heptane Oxidation," *Combustion and Flame* 114:149-177, 1998.
37. Westbrook, C. K., J. Warnatz and W. J. Pitz. *Eighteenth Syposium (International) on Combustion*, The Combustion Institute, pp. 749-767, 1981.
38. Westbrook, C. K., J. Warnatz and W. J. Pitz. *Twenty-Second Syposium (International) on Combustion*, The Combustion Institute, pp. 893-901, 1988.
39. Westbrook, C. K., W. J. Pitz and W. R. Leppard. "The Autoignition Chemistry of Paraffinic Fuels and Pro-Knock and Anti-Knock Additives: A Detailed Chemical Kinetic Study," SAE Technical Paper 912314, 1991.
40. Chevalier, C., W. J. Pitz, J. Warnatz, C. K. Westbrook and H. Melenk. *Twenty-Fourth Syposium (International) on Combustion*, The Combustion Institute, pp. 92-101, 1992.
41. Westbrook, C. K. and W. J. Pitz. Fall Meeting of the Western States Section of the Combustion Institute, Menlo Park, CA, October 18-20, 1993.
42. Wang, H. and M. Frenklach. "A Detailed Kinetic Modeling Study of Aromatics Formation in Laminar Premixed Acetylene and Ethylene Flames," Combustion and Flame 110:173-221, 1997.
43. Wang, H. and M. Frenklach. *Journal of Physical Chemistry* 98:11465-11489, 1994.
44. Wang, H. and M. Frenklach. *Journal of Physical Chemistry* 97:3867-3874, 1993.
45. Edgar, B. L., R. W. Dibble and D. W. Naegeli. "Autoignition of Dimethyl Ether and Dimethoxy Methane Sprays at High Pressures," SAE Technical Paper 971677, 1997.
46. Marinov, N. M, "A Detailed Chemical Kinetic Model for High Temperature Ethanol Oxidation," *International Journal of Chemical Kinetics* 31:183-220, 1999.
47. Shepherd, J. E. "CV" constant volume explosion structure calculation program, http://www.galcit.caltech.edu/EDL/public/codes.html.
48. Kee, Robert J., F. M. Rupley and J. A. Miller. "Chemkin-II: A FORTRAN Chemical Kinetics Packager for the Analysis of Gas-Phase Chemical Kinetics," Sandia Report SAND89-8009B, 1989.
49. Kee, Robert J., F. M. Rupley and J. A. Miller. "The Chemkin Thermodynamic Data Base," Sandia Report SAND87-8215B, 1990.
50. Hess, H. S., J. Szybist, A.L. Boehman, P.J.A. Tijm and F.J. Waller. "The Use of Cetaner for the Reduction of Particulate Matter Emissions in a Turbocharged Direct Injection Medium-Duty Diesel Engine," Seventeenth Annual International Pittsburgh Coal Conference, Pittsburgh, September 11-15, 2000.

DEFINITIONS, ACRONYMS, ABBREVIATIONS

0-D: zero-dimensional
^{14}C: carbon-14 radioisotope
AMS: accelerator mass spectrometry
CAD: crank angle degree
CN: cetane number
DEE: diethyl ether
DI: direct-injected
DME: dimethl ether
DMM: dimethoxy methane
HC: hydrocarbon
HR: heat release
NO_x: nitrogen oxides
NTC: negative temperature coefficient
NVOF: non-volatile organic fraction
PAH: polycyclic aromatic hydrocarbon
PM: particulate matter
ϕ: fuel-air equivalence ratio